

Towards advection on a full reduced grid for TM5

P.B. Hooghiemstra

KNMI Technical report = technisch rapport; TR-294

De Bilt, 2006

PO Box 201
3730 AE De Bilt
Wilhelminalaan 10
De Bilt
The Netherlands
<http://www.knmi.nl>
Telephone +31(0)30-220 69 11
Telefax +31(0)30-221 04 07

Author: Hooghiemstra, P.B. [Delft University of Technology]



Towards Advection on a Full Reduced Grid for TM5

P. B. Hooghiemstra¹

December 12, 2006

¹Delft University of Technology, department Electrical Engineering, Mathematics and Computer Science.

Contents

1	Introduction	3
2	Problem Definition	6
3	Grid Definition	7
3.1	Cell properties	7
3.2	Subgrid Tracer Distribution	8
3.3	Orthonormal Basis	9
4	One Dimensional Example	11
4.1	Advection Theory	11
4.2	Notation	14
4.3	Examples	15
4.3.1	A constant flux	15
4.3.2	A one sided zero-flux	16
4.3.3	A flow in two directions	17
5	General algorithm	19
5.1	Algorithm	19
5.2	Allocation of Mass	20
5.3	Mass Update	20
5.4	Determination of Distributions	21
5.4.1	Linear Mapping	23
5.5	Advection Summary	24
5.6	Applying Least Squares Method	24
6	Discussion	26
7	Conclusion	27
A	Linear Mapping	28
B	Least Squares Proof	30
C	Used Variables and Parameters	33

Chapter 1

Introduction

In this report we describe generalizations which have been made to the advection scheme of the TM5 chemistry-transport model. TM5 [Krol et al., 2005] is a global atmospheric model used by an international research community for the purpose of long range transport of chemical species and their subsequent effect on the regional atmosphere. The model is driven by meteorological fields originating from the IFS operational model used at ECMWF (European Center for Medium-range Weather Forecast). The data is stored offline as a pre-processed input and updated every 3 or 6 hours.

In the current implementation the TM5 model can either use the first-order slopes scheme [Russell and Lerner, 1981] or the second-order moments scheme [Prather, 1986], for the transport of tracers. The difference between these schemes is that less diffusive transport is calculated when using the second-order moments scheme, which is important for stratospheric studies. To model the advection, the finite volume method is used, which is natural for chemistry and has a high user acceptance. Finally, this method satisfies the underlying conservation of mass automatically. The advection uses a horizontal grid definition which is regular in both longitudinal (x) and latitudinal (y) direction known as a regular grid, see figure 1.1. The grid cells near the earth's poles have a much smaller area than those at the equator. For these smaller cells there is the possibility that during a model time-step more mass is advected out of a cell than the cell contains, the so called CFL (Courant, Friedrichs and Lewy) violation. In order to avoid this the time-step in the model must be reduced which is computationally expensive. A solution to this problem is the reduced grid [Petersen et al., 1998] where a number of smaller cells is combined into larger ones. That is, pole wards an integer number of cells from previous rows is combined. This is illustrated in figure 1.2. A drawback here is the relative big jump in the cell size from one latitudinal band to the other.

The original meteorological data originating from ECMWF is provided on a fully reduced grid. Figure 1.3 is an example of such a grid, where a variable

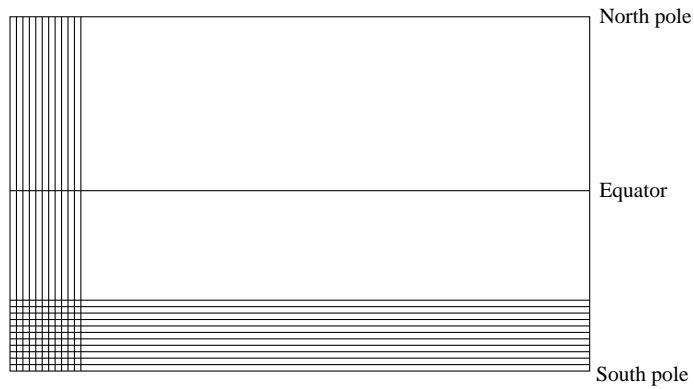


Figure 1.1: The regular grid on the earth in 2-D. The regular grid has on every latitude the same number of cells, they become smaller and smaller near the poles in terms of area.

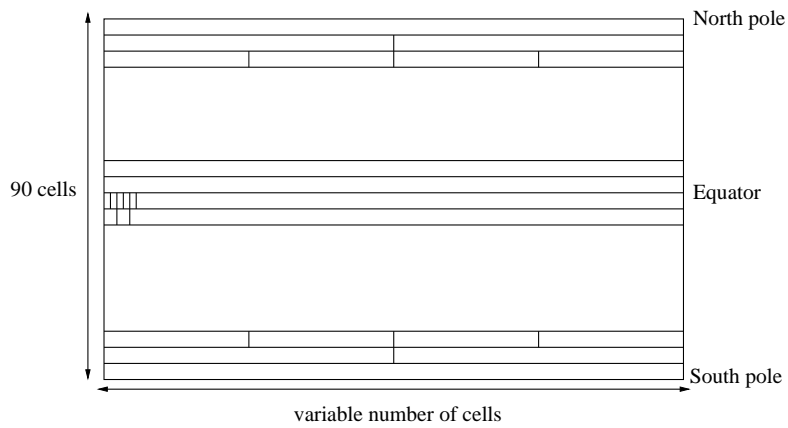


Figure 1.2: The reduced grid in 2-D. We see that the grid has only one cell at the poles and an increasing number of cells near and on the equator.

number of cells is included in the x direction. The cell length is constant within each row, but might differ from row to row. Since the data provided by ECMWF is on this type of grid it is desirable that the advection scheme also uses the fully reduced grid. However, for this to be feasible the advection scheme needs to be modified so that it performs well for such a grid. These grids on a sphere are illustrated in the appendix.

In chapter 2 we describe the problem. In chapter 3 we define the grid we

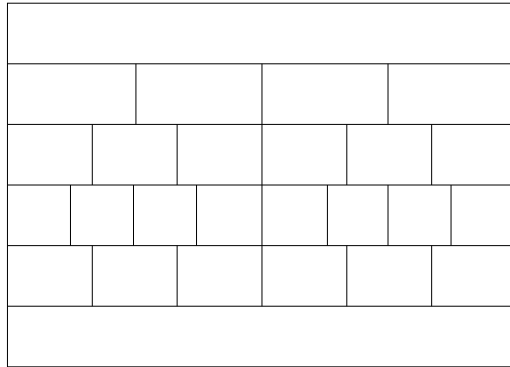


Figure 1.3: The fully reduced grid. We see that the grid is less structured than the former grids, which makes it possible to use lesser cells.

work on. Then, in chapter 4 we will start with the theory for the one dimensional case, followed by some examples. The general case will be treated in chapter 5. Chapter 6 contains some discussion about the theory. We end with the conclusion in section 7.

Chapter 2

Problem Definition

In summary, the definition of the problem is: *If the tracer distribution in a 2-D network of grid cells is known at time $t = t_0$, how do we achieve a valid approximation of the tracer distribution after a typical time step ($t = t_0 + \Delta t$)?*

Here we consider the advection of a passive tracer in a typical air-mass. A 2-D grid is adopted for this purpose (with advection in the x and y direction), where no vertical (z) advection is accounted for. In order to limit the computational cost we use the fully reduced grid (figure 1.3). We model the advection by considering the mass transfer which occurs to and from a particular grid cell. However, we must ensure that the advection accounts for multiple interactions by neighboring grid cells.

Before the advection is performed we assume that the tracer is distributed linearly throughout each grid cell. The mass of air [kg] in any cell is modified during the advection step of length Δt [s] by the prescribed fluxes [kg/s] on the cell edges. Due to these fluxes, tracer is transferred between cells which cause changes in the tracer distribution. Then we have multiple distributions defined on different parts of the cell. By some sort of averaging (least squares approximation) we have to make one distribution of these. We will come back to this in detail in the forthcoming sections.

We have a two dimensional problem here, so the advection occurs in two directions simultaneously. Because it is easier to do the advection in one direction at a time, we use operator splitting. We split the advection in a horizontal and a vertical part, in a symmetric way. The latter means that for one time step Δt we do the following subsequent steps: $X(\Delta t/2)$, $Y(\Delta t/2)$, $Y(\Delta t/2)$, $X(\Delta t/2)$, where X , Y are the advection operators in x and y direction respectively. The symmetric order reduces the error introduced by splitting [Lanser and Verwer, 1999]. Since the grid is regular in the x direction, the only difficult part is the modeling of the advection in the y direction, that is, the Y operator. That is the operator we will study here. The modeling of the advection in the x direction can be seen as a special case of the general advection in y direction.

Chapter 3

Grid Definition

Assume we are working on a full reduced grid. For explaining the mathematical model we will use figure 3.1. However, we start with listing some cell properties that we will use in the model.

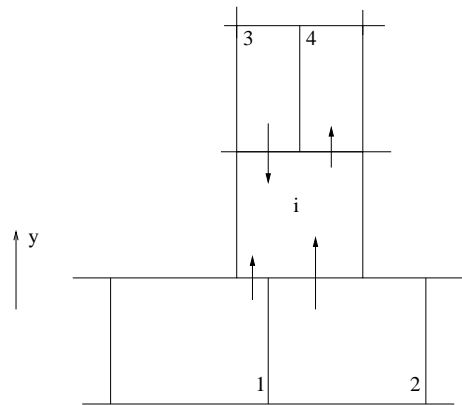


Figure 3.1: Zooming over the reduced grid.

3.1 Cell properties

In general we have a list of properties for each cell. These properties are for example: length, width, the number of neighbors, indices of neighbors and fluxes. All the cell properties are listed in table 3.1. Here we mean the following by inflow and outflow neighbors. An inflow neighbor is an adjacent cell of cell i for which during the advection step mass is transferred *into* cell i . An outflow neighbor is an adjacent cell for which mass is transferred *from* cell i . For

figure 3.1 this means that neighbors 1, 2 and 3 are inflow neighbors, and 4 is an outflow neighbor. The arrows indicate the amplitude and direction of the fluxes.

Property	Description	Unit
x_i	x-coordinaat center cell i ,	[m]
y_i	y-coordinaat center cell i ,	[m]
Δx_i	length cell i ,	[m]
Δy_i	height cell i ,	[m]
\mathcal{B}^i ,	collection of all neighbors	-
\mathcal{B}_{out}^i ,	collection of outflow neighbors	-
$no^i = \mathcal{B}_{out}^i $	# outflow neighbors	-
\mathcal{B}_{in}^i ,	collection of inflow neighbors	-
$ni^i = \mathcal{B}_{in}^i $	# inflow neighbors	-
\mathcal{B}_{low}^i ,	collection of lower neighbors indices	-
\mathcal{B}_{up}^i ,	collection of upper neighbors indices	-
$A_{in}^1, \dots, A_{in}^{ni_{low}}$	fluxes of all inflow neighbors	[kg/s]
$A_{out}^1, \dots, A_{out}^{no}$	fluxes of all outflow neighbors	[kg/s]
A^k	fluxes between cell i and k	[kg/s]

Table 3.1: List of properties of cell i .

In addition to the properties of cell i we need some information or properties of the neighbors of this cell. For every neighbor of cell i we need to know two things. The first one is the so-called *outward normal* n . This means that for a lower neighbor of i , $n = -1$ and for an upper neighbor we have $n = 1$. The second thing is if the neighbor is a full neighbor or partly a neighbor. This can be explained easily by considering figure 3.1 again. We see that neighbor 1 and 2 are only partly adjacent two cell i , so these are partly neighbors. Neighbors 3 and 4 on the other hand are full neighbors. Finally, we count the neighbors by starting by the lower left and we go from left to right.

3.2 Subgrid Tracer Distribution

In general we have within each grid cell a polynomial tracer distribution of degree n in two dimensions. We want to write the tracer distribution on a basis Φ of orthonormal functions on a *calculation* domain which is $[-\frac{1}{2}, \frac{1}{2}] \times [-\frac{1}{2}, \frac{1}{2}]$. In general we thus have

$$\Phi = \{\phi_0, \dots, \phi_n\}, \quad (3.1)$$

and we may write the tracer distribution in cell i as

$$f^i(x, y) = \sum_{j=0}^n \alpha_j^i \phi_j(x, y), \quad -\frac{1}{2} < x, y < \frac{1}{2}. \quad (3.2)$$

In this study however, we emphasis on a *linear* tracer distribution, hence $n = 2$.

3.3 Orthonormal Basis

We start with the construction of the orthonormal basis Φ for the innerproductspace $\mathbb{P}^1\left([-\frac{1}{2}, \frac{1}{2}] \times [-\frac{1}{2}, \frac{1}{2}]\right)$, from the standard basis $B = \{1, x, y\}$. That is, the space of all linear functions on the interval $[-\frac{1}{2}, \frac{1}{2}] \times [-\frac{1}{2}, \frac{1}{2}]$. The inner product is defined to be

$$\langle u, v \rangle = \int_{y=-\frac{1}{2}}^{\frac{1}{2}} \int_{x=-\frac{1}{2}}^{\frac{1}{2}} u(x, y)v(x, y) dx dy \quad \text{for } u, v \in \mathbb{P}^1. \quad (3.3)$$

By using the orthogonalizing algorithm from Gram-Schmidt [Lay, 2003], with some normalizing in addition, we obtain our desired basis

$$\Phi := \{\phi_0, \phi_1, \phi_2\} = \left\{ 1, 2\sqrt{3}x, 2\sqrt{3}y \right\}. \quad (3.4)$$

Such that for the elements of Φ holds

$$\langle \phi_i, \phi_j \rangle = \delta_{ij} = \begin{cases} 1, & i = j, \\ 0, & i \neq j \end{cases} \quad (3.5)$$

Figure 3.2 illustrates the subgrid tracer distribution for the one dimensional case which we will treat in the next chapter, where we count the neighbors as we defined in section 3.1.

The chosen basis has a few advantages. The domain $[-\frac{1}{2}, \frac{1}{2}] \times [-\frac{1}{2}, \frac{1}{2}]$ is symmetric around zero, so the middle point of the domain is 0, which is easier and more readable then in case of an unsymmetric interval. In the end we have to say that it doesn't matter which interval we take if we use it in a consequent way, but there are some choices that makes life easy.

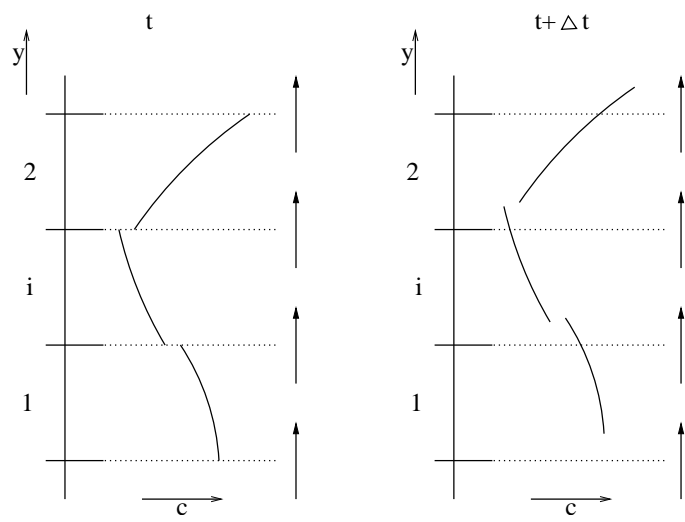


Figure 3.2: Definition of the tracer distribution with constant flux in a vertical flow. Tracer distributions are blown up from below.

Chapter 4

One Dimensional Example

Assume that we have a situation as in the left part of figure 4.1. Here we see one dimensional flow in the y direction. Let us furthermore assume for now that the fluxes are equal to each other.

4.1 Advection Theory

A first step in the numerical advection process is to define the new cell mass due to fluxes through the edges of cell i . Assume that the mass on time t is written $m_i(t)$. The new mass a time step Δt later can be described using table 3.1 by

$$m_i(t + \Delta t) = m_i(t) - \sum_{k \in \mathcal{B}^i} A^k \Delta t n(k). \quad (4.1)$$

Now the air mass has been updated, we consider the advection of the tracer itself. In general we have inflow or outflow on both edges of the cell, so we split cell i in 3 parts. In this simple example we have inflow on the lower edge and outflow on the upper edge (figure 4.1). The lower part (a) is used for the distribution of the lower inflow neighbor. The middle part (b) is used for the tracer remaining in the cell. The rest of the cell (c) flows out of cell i , and is not of that much interest, although we need to know how much air (with tracer) is blown out of cell i . So we will start with the latter one.

The total net outflow mass leaving cell i through the upper edge is

$$\Delta m_{out;up}^i = - \sum_{k \in \mathcal{B}_{up}^i \cap \mathcal{B}_{out}^i} A_{out}^k \Delta t n(k). \quad (4.2)$$

The fraction of the air mass that left cell i is

$$e_U = \frac{\Delta m_{out;up}^i}{m_i(t)} \in [0, 1]. \quad (4.3)$$

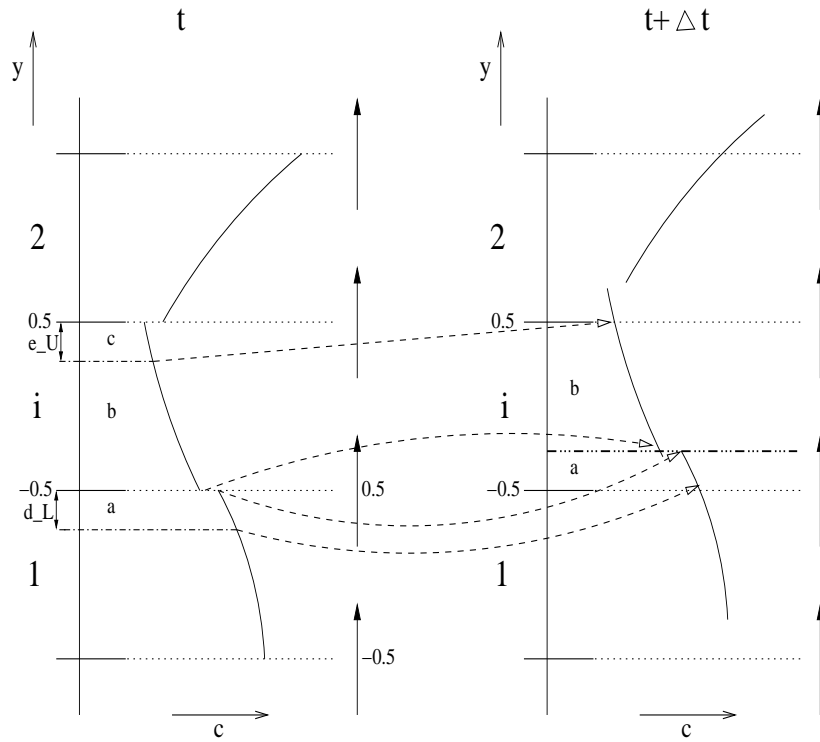


Figure 4.1: Tracer distribution on the subgrid in three adjacent cells before advection with the in and outflow fractions d_L and e_U (left). During advection cell i is divided in two parts (a and b), separated by the tripple dots line. The lower part (a) is for the distribution of the tracer that is blown into the cell. The remaining part (b) is for the distribution of tracer that remains in the cell (right). The dotted arrows give an indication of the mapping. The neighbors of cell i are counted as defined in the last chapter.

Here we have

$$e_U = \frac{A_{out}^2 \Delta t}{m_i(t)}. \quad (4.4)$$

Then we turn our attention to the inflow into cell i from below. The total net inflow mass entering cell i is

$$\Delta m_{in;low}^i = - \sum_{k \in \mathcal{B}_{low}^i \cap \mathcal{B}_{in}^i} A_{in}^k \Delta t n(k). \quad (4.5)$$

The fraction of the air mass that entered cell i through the lower edge is

$$d_U = \frac{\Delta m_{in;low}^i}{m_i(t + \Delta t)}, \quad (4.6)$$

which, in this case is equal to

$$d_U = \frac{A_{in}^1 \Delta t}{m_i(t + \Delta t)}. \quad (4.7)$$

With this mass there is also tracer advected in cell i . But the part of the cell from where the tracer originates, is defined on the upper part of cell 1, (see left side of figure 4.1). We map this function such that it is defined on the lower part of cell i . We also require tracer mass conservation. Remember that per cell we work on our *calculation* domain $[-\frac{1}{2}, \frac{1}{2}] \times [-\frac{1}{2}, \frac{1}{2}]$. So it is not sufficient only to translate the part of the distribution of the inflow tracer, because we would leave the calculation domain. Therefore we have to map the distribution in the following way (figure 4.1, block a).

$$\hat{f}^1(x, y) = \rho^1 f^1(x, \rho^1(y - \zeta^1)), \quad -\frac{1}{2} < x < \frac{1}{2}, \quad -\frac{1}{2} < y < -\frac{1}{2} + d_L, \quad (4.8)$$

where ρ^1, ζ^1 are provided by the Lin-Map function defined in chapter 5

$$[\rho^1, \zeta^1] = \text{Lin-Map}\left(\frac{1}{2} - d_L, \frac{1}{2}, -\frac{1}{2}, -\frac{1}{2} + d_L\right). \quad (4.9)$$

We may actually prove the mass conservation by considering that

$$\int_{x=-\frac{1}{2}}^{\frac{1}{2}} \int_{y=-\frac{1}{2}}^{-\frac{1}{2}+d_L} \hat{f}^1(x, y) dx dy = \int_{x=-\frac{1}{2}}^{\frac{1}{2}} \int_{y=-\frac{1}{2}}^{-\frac{1}{2}+d_L} \rho^1 f^1(x, \rho^1(y - \zeta^1)) dx dy. \quad (4.10)$$

If we now substitute $\nu = \rho^1(y - \zeta^1)$, and work out the details we find that the latter integral in (4.10) is equal to

$$\int_{x=-\frac{1}{2}}^{\frac{1}{2}} \int_{\nu=\frac{1}{2}-d_L}^{\frac{1}{2}} f^1(x, \nu) dx d\nu. \quad (4.11)$$

And this is exactly the mass of the tracer that is blown into cell i .

Then we turn to the part of the tracer distribution that remains in cell i . We already know how much air is blown out, and what fraction of the total mass it is, so we may directly apply the mapping (figure 4.1, block b)

$$\tilde{f}^i(x, y) = \rho^r f^i(x, \rho^r(y - \zeta^r)), \quad -\frac{1}{2} < x < \frac{1}{2}, \quad -\frac{1}{2} + d_L < y < \frac{1}{2}, \quad (4.12)$$

where

$$[\rho^r, \zeta^r] = \text{Lin-Map}\left(-\frac{1}{2}, \frac{1}{2} - e_U, -\frac{1}{2} + d_L, \frac{1}{2}\right) \quad (4.13)$$

Now we have a piecewise linear tracer concentration \bar{f} defined in cell i . We write the piecewise function \bar{f} as

$$\bar{f}(x, y) = \begin{cases} \hat{f}^1(x, y), & -\frac{1}{2} < x < \frac{1}{2}, \quad -\frac{1}{2} < y < -\frac{1}{2} + d_L, \\ \tilde{f}^i(x, y), & -\frac{1}{2} < x < \frac{1}{2}, \quad -\frac{1}{2} + d_L < y < \frac{1}{2}. \end{cases} \quad (4.14)$$

We construct a function g by

$$g(x, y) = \sum_{j=0}^2 \beta_j \phi_j(x, y), \quad -\frac{1}{2} < x, y < \frac{1}{2}, \quad (4.15)$$

By applying the method of least squares we can choose the coefficients β_j such that the difference is minimal in l_2 sense.

$$I = \int_{-\frac{1}{2}}^{\frac{1}{2}} \int_{-\frac{1}{2}}^{\frac{1}{2}} [\bar{f}(x, y) - g(x, y)]^2 dx dy. \quad (4.16)$$

The expression for the coefficients β_j is (for the proof see appendix B)

$$\beta_j = \int_{-\frac{1}{2}}^{\frac{1}{2}} \int_{-\frac{1}{2}}^{\frac{1}{2}} \bar{f}(x, y) \phi_j(x, y) dx dy, \quad \text{for } j = 0, 1, 2. \quad (4.17)$$

4.2 Notation

We saw in the example of the advection scheme in section 4.1 for the most simple case that we need some notational conventions to keep things readable and understandable. We introduce the following notation. Before we do any advection we have a tracer distribution in all cells, denoted by

$$f^l(x, y) = \sum_{j=0}^2 \alpha_j^l \phi_j(x, y), \quad -\frac{1}{2} < x, y < \frac{1}{2} \quad \text{and } l = 1, \dots, N_{tot} \quad (4.18)$$

where N_{tot} is the total number of cells. During the advection step we have to map the distributions of the inflow neighbors. These neighbors are numbered $1, \dots, ni$ and the mapped functions will be denoted by $\hat{f}^k(x, y)$ for $k = 1, \dots, ni$. The mapping parameters we use (ρ and ζ) are denoted by $\rho_{in}^k, \zeta_{in}^k$. Then we have to map the part of the tracer distribution that remains in the cell under consideration (we assume this is cell i). We denote this mapped distribution by $\tilde{f}^i(x, y)$, the mapping parameters are ρ_r, ζ_r .

After we have accomplished all the mappings we have to do a least squares approximation. We build a piecewise linear function and denote it by $\bar{f}(x, y)$. Finally we obtain a continuous fit to this piecewise function which we will call $g(x, y)$.

If we have to write the functions in terms of linear combinations of basis functions, we apply the same notation for the coefficients as for the functions itself. This means, for example, that we write

$$\bar{f}(x, y) = \sum_{j=0}^2 \bar{\alpha}_j \phi_j(x, y), \quad -\frac{1}{2} < x, y < \frac{1}{2}. \quad (4.19)$$

Furthermore, the coefficients of the function g are chosen to be β_j . A whole list of used variables and constants can be found in appendix C.

4.3 Examples

In this section we want to illustrate the theory of the former sections. We show a number of one dimensional examples with different fluxes to show different situations. The grid consists of $N_{tot} = 10$ cells and is uniform with cell length $\Delta x = 1$. We will start with a constant flux on the whole domain ($0 \leq x \leq 10$.) After that we will show what happens if a flux is chosen zero somewhere. Finally we will show the consequence of a varying flux through the domain. In all examples we consider periodic boundary conditions, and an initial air mass of 100 kg in every cell. The first two examples assume a tracer mass of 1 kg in cell 1, the last example assumes a tracer mass of 1 kg in cells 5 and 7.

4.3.1 A constant flux

We define all the fluxes to be equal: 10 kg/s and one timestep is 1 s . We will only show figures of the tracer mass, since the air mass is constant.

We see that there is nothing spectacular. The tracer is transported through the domain and spreads out (diffusion). See figure 4.2.

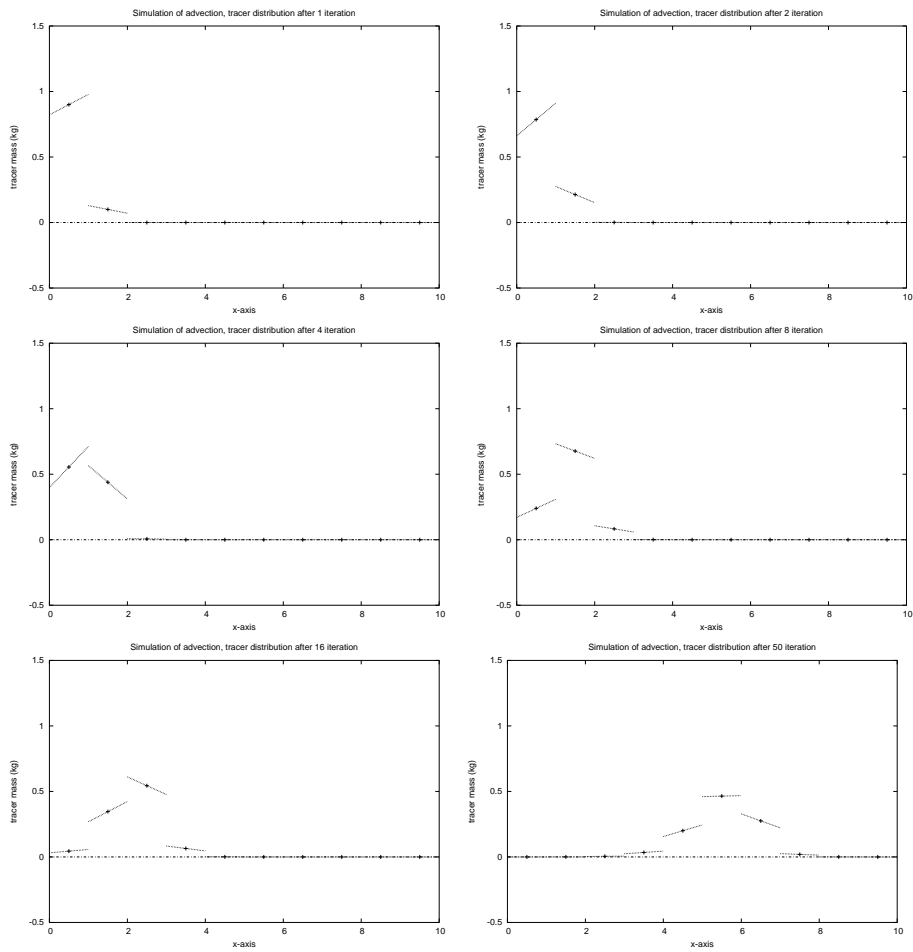


Figure 4.2: The tracer mass simulated after 1, 2, 4, 8, 16 and 50 iterations respectively, with constant flux.

4.3.2 A one sided zero-flux

In this example we define all fluxes to be 10 kg/s , but there is no flux out of cell 2. We expect that the tracer mass is transported to the second cell and remains there.

In figure 4.3 we see things happen as we expected. But after a number of timesteps we can't simulate further since the air mass in cell 3 is getting negative. This is the case because there is a negative net mass transfer in this cell. We have build in an error exception that aborts the simulation as soon as this happens.

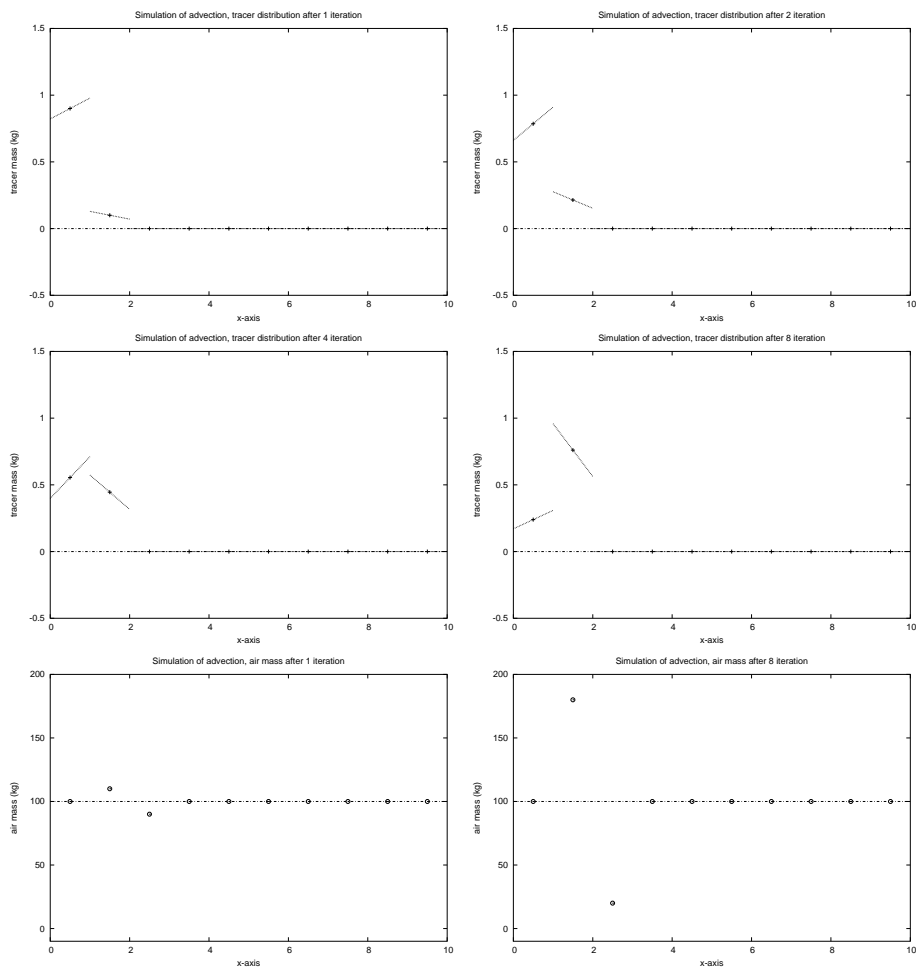


Figure 4.3: The tracer mass simulated after 1 and 2 iterations, with no flux out of cell 2. The lowest two figures represent the air mass per cell.

4.3.3 A flow in two directions

In the last example we take a flow in two directions. We start with a tracer mass of 1 kg in cells 5 and 7. Then we define our flux in such a way that there is a flow out of these two cells into their adjacent ones. But we have a zero flux at the left of cell 4 and at the right of cell 8, because this illustrates this example better. The figures are shown in 4.4.

We see that the cells 4, 6 and 8 fill up with tracer, where cell 6 fills up faster since it has inflow from both sides. Again we can't simulate more since the air

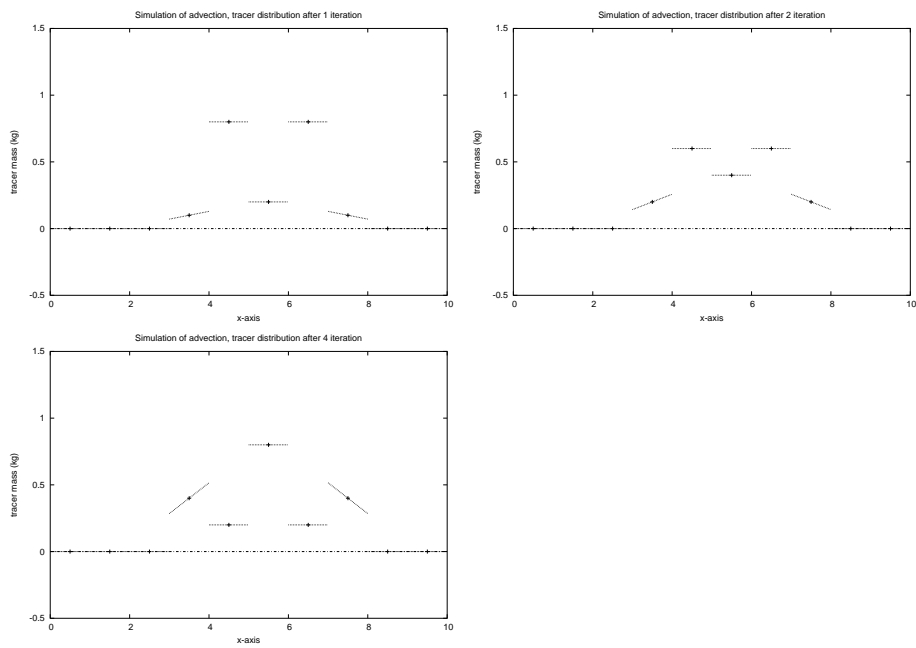


Figure 4.4: The tracer mass after 1, 2 and 4 iterations. We start with 1 kg tracer in cells 5 and 7 and choose the flux such that there is a flow in two directions out of these cells. There is no flux out of cells 4 and 8.

mass is becoming negative then in cells 5 and 7.

Chapter 5

General algorithm

Now we consider the general case of vertical advection on a fully reduced grid. The situation is as in figure 5.1. Several steps have to be taken to do the advection step, which will be stated below and explained in detail in the forthcoming sections.

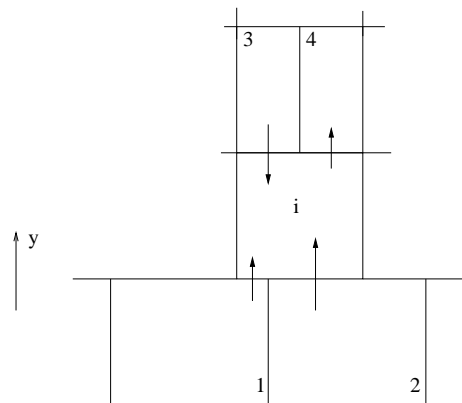


Figure 5.1: Zooming over the reduced grid.

5.1 Algorithm

We note that we have to distinguish between two kinds of updates for implementation. The first is a general update for all the cells, the second is a cell by cell update. The following steps can be performed for all cells at once.

1. Compute the new cell mass $m(t + \Delta t)$.

2. Compute the total lower outflow mass e_L .
3. Compute the total upper outflow mass e_U .
4. Compute the total lower inflow mass d_L .
5. Compute the total upper inflow mass d_U .

Now we know the new mass and the in and outflow mass for all cells, we loop over all the cells. For each cell the following steps are taken

6. Use the values of e_L which were computed in step 2 to divide the inflow neighbors and cell i itself in remaining and outflow parts
7. Determine for the inflow neighbors from which cell they originate (outflow from this cell) and which parts flow in where.
8. Do the same for the upper inflow neighbors.
9. Apply the appropriate mapping.
10. Map the tracer distribution for the remaining part.
11. Apply least squares to obtain a continuous tracer distribution in cell i .

5.2 Allocation of Mass

We start with a visual explanation of the algorithm. Here we only emphasize on the question 'If a part of a cell is advected, where is it a time step later?' Figure 5.2 (left) shows a part of the grid with for each cell the outflow blocks. The right part shows the inflow blocks for each cell. If we now number the outflow blocks, then we can easily see where they are after advection. However we must be careful in case of a cell with double in or outflow. Assume we have double outflow from a cell (The cell with the blocks 2 and 3 in the left part of figure 5.2). Then we have to determine which part of the outflow block flows in where using the fluxes. In this case we divide the outflow block in two parts. The greatest flux will advect the most mass, hence this part must be bigger. Note that we only numbered some blocks in figure 5.2, since this is only a small example to explain the steps we will take.

5.3 Mass Update

We can update the mass (step 1) for every cell, since we know the neighbors (\mathcal{B}^i) and the prescribed fluxes (A). From equation (4.1) we obtain

$$m_i(t + \Delta t) = m_i(t) - \sum_{k \in \mathcal{B}^i} A^k \Delta t n(k). \quad (5.1)$$

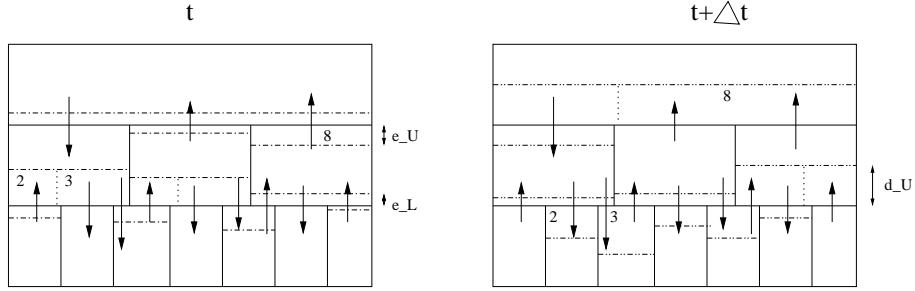


Figure 5.2: The outflow (left) and inflow (right) diagram. Here we show where the different parts of a new cell originate from. We see that blocks 2, 3 and 8 are advected to another cell.

For the transfer of mass we start with the outgoing mass through the lower edge. We compute this by

$$\Delta m_{out;low}^i = - \sum_{k \in \mathcal{B}_{out}^i \cap \mathcal{B}_{low}^i} A_{out}^k \Delta t n(k). \quad (5.2)$$

The fraction of the cell that flows out (step 2) is then defined by

$$e_L = \frac{\Delta m_{out;low}^i}{m_i(t)}. \quad (5.3)$$

Idem for the mass transfer through the upper edge (step 3). Then we compute the total mass incoming (step 4) through the lower edge by

$$\Delta m_{in;low}^i = - \sum_{k \in \mathcal{B}_{in}^i \cap \mathcal{B}_{low}^i} A_{in}^k \Delta t n(k). \quad (5.4)$$

The fraction of cell i to be filled with parts of the distributions of the lower inflow neighbors is d_L and this number is defined by

$$d_L = \frac{\Delta m_{in;low}^i}{m_i(t + \Delta t)}, \quad (5.5)$$

For the upper inflow neighbors we do exactly the same (step 5).

5.4 Determination of Distributions

Assume that cell i has n outgoing fluxes on the lower edge (hence this block is divided in n parts: one for each neighbor) as illustrated in figure 5.3 for $n = 2$. The fluxes are numbered A^1, \dots, A^n . Every flux determines the size of a part

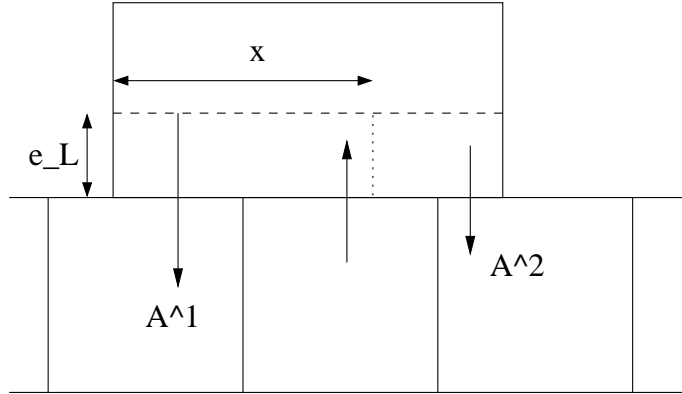


Figure 5.3: The parting of an outflow block in two pieces, depending on the size of the fluxes. Here we have $x = |A^1| \Delta t / \Delta m_{out;low}^i$.

of the block that is advected (step 6). For flux number l we get the following part of the original outflow block

$$[c_{l-\frac{1}{2}}, c_{l+\frac{1}{2}}], \quad (5.6)$$

where

$$c_{l-\frac{1}{2}} = -\frac{1}{2} + \frac{\sum_{j=1}^{l-1} |A^j| \Delta t}{\Delta m_{out;low}^i}, \quad (5.7)$$

$$c_{l+\frac{1}{2}} = c_{l-\frac{1}{2}} + \frac{|A^l| \Delta t}{\Delta m_{out;low}^i}. \quad (5.8)$$

For the example in figure 5.3 we have $c_{2-\frac{1}{2}} = -\frac{1}{2} + x$.

Next we consider an inflow block of n incoming fluxes, also on the lower edge, which is illustrated in figure 5.4 for $n = 5$. Again we have to compute the size of the different parts (step 7) depending on the fluxes. We obtain for flux number k

$$[a_{k-\frac{1}{2}}, a_{k+\frac{1}{2}}], \quad (5.9)$$

where

$$a_{k-\frac{1}{2}} = -\frac{1}{2} + \frac{\sum_{j=1}^{k-1} A_l^j \Delta t}{\Delta m_{in;low}^i}, \quad (5.10)$$

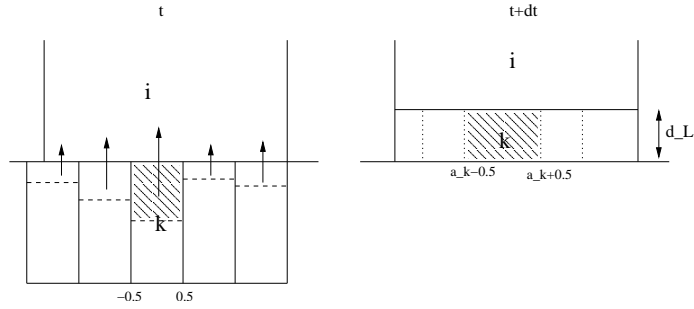


Figure 5.4: The k^{th} lower inflow neighbor is advected into cell i . We have to map the tracer distribution in order to apply the least squares method later on.

$$a_{k+\frac{1}{2}} = a_{k-\frac{1}{2}} + \frac{A_l^k \Delta t}{\Delta m_{in;low}^i}. \quad (5.11)$$

Again everything we did in this section also holds for the upper edge of cell i (step 8).

5.4.1 Linear Mapping

Now we know which part of the tracer distribution of an inflow neighbor comes where in cell i , we must map (step 9) the functions to be able to perform the least squares method in the next subsection. Figure 5.4 illustrates the advection of the k^{th} lower inflow neighbor. We divide the mapping in two parts: the mapping in x- and in y-direction respectively. The mapping in x-direction is given by Lin-Map

$$[\lambda, \xi] = \text{Lin-Map}(x_1, x_2, \tilde{x}_1, \tilde{x}_2). \quad (5.12)$$

If we look at the left part of figure 5.5 where we see the mapping in detail, we see that the input for the linear mapping in this case is $x_1 = -\frac{1}{2}$, $x_2 = \frac{1}{2}$, $\tilde{x}_1 = a_{k-\frac{1}{2}}$ and $\tilde{x}_2 = a_{k+\frac{1}{2}}$.

The mapping in y-direction is illustrated in the right part of figure 5.2, which is given by

$$[\rho, \zeta] = \text{Lin-Map}(y_1, y_2, \tilde{y}_1, \tilde{y}_2), \quad (5.13)$$

The input for this mapping is $y_1 = \frac{1}{2} - z^k$, $y_2 = \frac{1}{2}$, $\tilde{y}_1 = -\frac{1}{2}$ and $\tilde{y}_2 = -\frac{1}{2} + d_L$, where z^k is defined as the fraction of mass the flux A^k blows into cell i .

Note that in case of a partial lower neighbor, that is, a neighbor that has two upper neighbors, the input for the linear mapping changes a bit. For a full

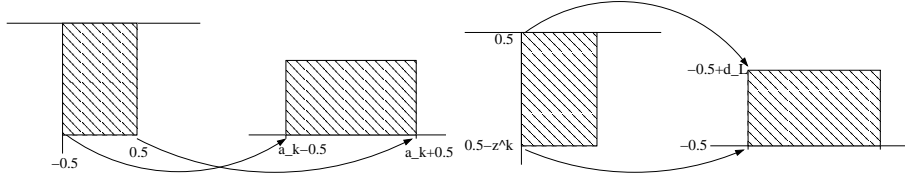


Figure 5.5: The linear mapping in x (left) and y (right) direction. Here we have $z^k = A^k \Delta t / m_i(t + \Delta t)$.

neighbor we always have $x_1 = -\frac{1}{2}$ and $x_2 = \frac{1}{2}$. For a partial neighbor on the left side we get $x_1 = \frac{1}{2} - \text{part}_1$ while x_2 is unchanged. For a right partial neighbor we obtain $x_2 = -\frac{1}{2} + \text{part}_n$ and in this case x_1 is unchanged.

5.5 Advection Summary

What do we have now? We have mapped the tracer distributions of the inflow neighbors in such a way that we may apply a least squares approximation. We thus have for the lower inflow neighbor k

$$\hat{f}^k(x, y) = \lambda^k \rho^k f^k(\lambda^k(x - \xi^k), \rho^k(y - \zeta^k)), \quad a_{k-\frac{1}{2}} < x < a_{k+\frac{1}{2}}, \quad -\frac{1}{2} < y < -\frac{1}{2} + d_L. \quad (5.14)$$

For the upper inflow neighbors this whole derivation is analogue.

The last thing we have to do, is to map the distribution of the part of the tracer that remains in cell i (step 10). Due to outflow out of this cell (e_L, e_U) the mapping arguments are

$$[\rho_r, \zeta_r] = \text{Lin-Map}\left(-\frac{1}{2} + e_L, \frac{1}{2} - e_U, -\frac{1}{2} + d_L, \frac{1}{2} - d_U\right). \quad (5.15)$$

5.6 Applying Least Squares Method

After all the mappings we have a piecewise linear distribution in cell i . We write

$$\bar{f}(x, y) = \begin{cases} \hat{f}^1(x, y), & -\frac{1}{2} < x < a_{1+\frac{1}{2}}, & -\frac{1}{2} < y < -\frac{1}{2} + d_L, \\ \vdots & \vdots & \vdots \\ \hat{f}^n(x, y), & a_{n-\frac{1}{2}} < x < \frac{1}{2}, & -\frac{1}{2} < y < -\frac{1}{2} + d_L, \\ \tilde{f}^i(x, y), & -\frac{1}{2} < x < \frac{1}{2}, & -\frac{1}{2} + d_L < y < \frac{1}{2} - d_U, \\ \hat{f}^{n+1}(x, y), & -\frac{1}{2} < x < b_{1+\frac{1}{2}}, & \frac{1}{2} - d_U < y < \frac{1}{2}, \\ \vdots & \vdots & \vdots \\ \hat{f}^{ni}(x, y), & b_{ni-n-\frac{1}{2}} < x < \frac{1}{2}, & \frac{1}{2} - d_U < y < \frac{1}{2}, \end{cases}$$

Then we want to approximate this function \bar{f} with a continuous one (step 11), we name it g

$$g(x, y) = \sum_{j=0}^2 \beta_j \phi_j(x, y), \quad -\frac{1}{2} < x, y < \frac{1}{2}. \quad (5.16)$$

We choose the coefficients β_j such that the integral

$$I = \int_{-\frac{1}{2}}^{\frac{1}{2}} \int_{-\frac{1}{2}}^{\frac{1}{2}} [\bar{f}(x, y) - g(x, y)]^2 dx dy, \quad (5.17)$$

is minimal, see appendix B. The expression for the coefficients β_j is then

$$\beta_j = \int_{-\frac{1}{2}}^{\frac{1}{2}} \int_{-\frac{1}{2}}^{\frac{1}{2}} \bar{f}(x, y) \phi_j(x, y) dx dy, \quad \text{for } j = 0, 1, 2. \quad (5.18)$$

If we really want to calculate the coefficients β we have to split the integral in (5.18) into $ni + 1$ pieces, since we have that much discontinuities. If we do this, we see in the end that we only need integrals I of the form:

$$I(a, b, c, d, \rho^k, \zeta^k, \lambda^k, \xi^k) = \int_{x=a}^b \int_{y=c}^d \phi_i(\lambda^k(x - \xi^k), \rho^k(y - \zeta^k)) \phi_j(x, y) dx dy. \quad (5.19)$$

Since the ϕ_j are polynomials in x and y , analytical expressions for these integrals can be derived. To avoid mistakes, our advise is to use a computer algebra package like Maple for this.

Chapter 6

Discussion

The question is, now we have finished the algorithm, does it always work? There might be some (one or more) cases in which the algorithm fails.

One possibility is a flux that is so large that there is more mass advected than there originally was in that cell (CFL-violation). This is not possible ofcourse, since the time step Δt is chosen in such a way that prevent this to occur.

Another thing that we did not mention yet, is the presence of boundary conditions. To handle these (periodic) conditions, we place a set of halo cells all around the grid and define appropriate fluxes through the cell edges. This enables us to implement the algorithm more easily, since we don't have to worry about transferred air mass from the left to the right boundary. We have to be careful to update these halo cells every timestep, with the properties of their originals on the other side of the grid. Note that the introduction of halo cells only works if we prescribe the right fluxes for this cells.

We must also mention here that our choice of subdividing the in and outflow blocks in rectangles is quite random. We could have chosen it another way around, but this choice has been made for implementation reasons. If we keep working with rectangular cells and partitionings this is more easy.

The final remark which has already been tipped of in the introduction is about the dimensional reduction. In general we are working in three dimensions. Since we assume that in the vertical (z) direction we have one dimensional columns of grid cells, we may do this advection over the whole grid at once.

Chapter 7

Conclusion

In this report we proposed a more efficient method for advection which can be used in the chemical transport model TM5. Therefore we have introduced a full reduced grid on which we do not have to limit the time step in certain regions, which was the case in the old situation. The advection scheme itself became rather complicated since we have multiple interactions between cells during a time step. These interactions are caused by the different number of cells on each row in the full reduced grid.

With the introduction of orthonormal polynomial tracer distributions in each grid cell, we have generalized the description of the subgrid concentration. The orthonormal basis Φ we build for the space of linear functions of two variables (\mathbb{P}^1), makes it easy to find or map new distributions, using the Lin-Map operator. Another thing is, that it is easily extended to more than just linear functions. For example, we can do the second-order moments by adding some extra orthonormal basis functions to Φ . The advection itself is fully governed by the in and outflow blocks as illustrated by figure 5.2. The placement of in-/outflow blocks is a matter of bookkeeping for cells with a lot of neighbors.

We have seen that with the full reduced grid it is not necessary anymore to use very small time steps near the poles. This is good for the advection, since it can be solved more quickly. On the other hand, we have more work to do every timestep as mentioned in section 4.

Appendix A

Linear Mapping

In chapters 4 and 5 we have introduced a linear mapping, without explaining in detail what it does. So we will do this here. The mapping is called Lin-Map and maps the line segment on the x axis through the points x_1 and x_2 to the line segment on the y axis through points χ_1 and χ_2 . This map is defined by

$$[\lambda, \mu] = \text{Lin-Map}(x_1, x_2, \chi_1, \chi_2), \quad (\text{A.1})$$

and this is illustrated in figure A.1.

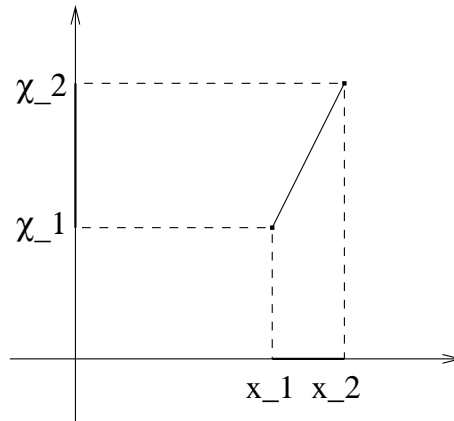


Figure A.1: The linear mapping maps a straight line segment between points x_1 and x_2 to the line segment between χ_1 and χ_2 .

The mapping parameters λ , μ are obtained by solving the equations

$$\begin{aligned} x_1 &= \lambda(\chi_1 - \mu), \\ x_2 &= \lambda(\chi_2 - \mu). \end{aligned}$$

Solving yields

$$\lambda = \frac{x_1 - x_2}{\chi_1 - \chi_2},$$
$$\mu = \chi_1 - \frac{x_1}{\lambda}.$$

Note that these parameters are always well defined. It is not possible to have a division by zero since χ_1 and χ_2 are never the same.

Appendix B

Least Squares Proof

In chapters 4 and 5 we did not prove that our function g is really the least squares approximation to the discontinuous function \bar{f} . We will prove this here for the case that there is only one discontinuity, in the point $y = c$.

Theorem 1 (Least Squares) *Suppose \bar{f} is a piecewise linear function on $[-\frac{1}{2}, \frac{1}{2}]^2$ of the form*

$$\bar{f}(x, y) = \begin{cases} \hat{f}(x, y), & -\frac{1}{2} < x < \frac{1}{2}, -\frac{1}{2} < y < c, \\ \tilde{f}(x, y), & -\frac{1}{2} < x < \frac{1}{2}, c < y < \frac{1}{2}, \end{cases} \quad (\text{B.1})$$

where $c \in [-\frac{1}{2}, \frac{1}{2}]$ and \hat{f}, \tilde{f} are defined by

$$\hat{f}(x, y) = \sum_{j=0}^2 \hat{\alpha}_j \phi_j(x, y), \quad -\frac{1}{2} < x < \frac{1}{2}, -\frac{1}{2} < y < c \quad (\text{B.2})$$

$$\tilde{f}(x, y) = \sum_{j=0}^2 \tilde{\alpha}_j \phi_j(x, y), \quad -\frac{1}{2} < x < \frac{1}{2}, c < y < \frac{1}{2}. \quad (\text{B.3})$$

$$(\text{B.4})$$

If we want to approximate \bar{f} by a continuous function g written as

$$g(x, y) = \sum_{j=0}^2 \hat{\beta}_j \phi_j(x, y), \quad -\frac{1}{2} < x, y < \frac{1}{2}, \quad (\text{B.5})$$

that satisfies

$$g(x, y) = \min_{g^* \in \mathbb{P}^1} \int_{-\frac{1}{2}}^{\frac{1}{2}} \int_{-\frac{1}{2}}^{\frac{1}{2}} [g^*(x, y) - \bar{f}(x, y)]^2 dx dy, \quad (\text{B.6})$$

then we have to choose the constants β_j as

$$\beta_j = \int_{-\frac{1}{2}}^{\frac{1}{2}} \int_{-\frac{1}{2}}^{\frac{1}{2}} \bar{f}(x, y) \phi_j(x, y) dx dy \quad \text{for } j = 0, 1, 2. \quad (\text{B.7})$$

Proof : Assume that we can write \bar{f} as in equation (B.1) and consider the integral

$$I = \int_{-\frac{1}{2}}^{\frac{1}{2}} \int_{-\frac{1}{2}}^{\frac{1}{2}} [\bar{f}(x, y) - g(x, y)]^2 dx dy. \quad (\text{B.8})$$

We write g as in equation (B.5) where the coefficients (β_j) are unknown (for now). Then g is our desired minimum of I for $\frac{\partial I}{\partial \beta_j} = 0$. Let us write the expression for I out in detail and compute the derivatives after that, using the discription of equation (B.2) and (B.3) for \bar{f} . We then find

$$\begin{aligned} I &= \int_{-\frac{1}{2}}^{\frac{1}{2}} \int_{-\frac{1}{2}}^{\frac{1}{2}} g^2(x, y) + \bar{f}^2(x, y) - 2\bar{f}(x, y)g(x, y) dx dy \\ &= \int_{-\frac{1}{2}}^{\frac{1}{2}} \int_{-\frac{1}{2}}^{\frac{1}{2}} g^2(x, y) + \bar{f}(x, y) \left(\bar{f}(x, y) - 2g(x, y) \right) dx dy \end{aligned}$$

Since we have orthonormal functions, this then yields

$$I = \sum_{j=0}^2 \beta_j^2 + \int_{-\frac{1}{2}}^{\frac{1}{2}} \int_{-\frac{1}{2}}^{\frac{1}{2}} \bar{f}(x, y) \left(\bar{f}(x, y) - 2 \sum_{j=0}^2 \beta_j \phi_j(x, y) \right) dx dy. \quad (\text{B.9})$$

Next we split up the integral in two pieces because \bar{f} is discontinuous in $y = c$, yielding

$$\begin{aligned} I &= \sum_{j=0}^2 \beta_j^2 + \int_{x=-\frac{1}{2}}^{\frac{1}{2}} \int_{y=-\frac{1}{2}}^c \hat{f}(x, y) \left(\hat{f}(x, y) - 2 \sum_{j=0}^2 \beta_j \phi_j(x, y) \right) dx dy \\ &+ \int_{x=-\frac{1}{2}}^{\frac{1}{2}} \int_{y=c}^{\frac{1}{2}} \tilde{f}(x, y) \left(\tilde{f}(x, y) - 2 \sum_{j=0}^2 \beta_j \phi_j(x, y) \right) dx dy. \end{aligned}$$

If we now differentiate I with respect to β_j and set this equal to zero we get

$$\frac{\partial I}{\partial \beta_j} = 2\beta_j + \int_{x=-\frac{1}{2}}^{\frac{1}{2}} \int_{y=-\frac{1}{2}}^c -2\hat{f}(x, y) \phi_j(x, y) dx dy$$

$$+ \int_{x=-\frac{1}{2}}^{\frac{1}{2}} \int_{y=c}^{\frac{1}{2}} -2\tilde{f}(x, y) \phi_j(x, y) dx dy = 0.$$

And hence we obtain

$$\beta_j = \int_{-\frac{1}{2}}^{\frac{1}{2}} \int_{-\frac{1}{2}}^{\frac{1}{2}} \bar{f}(x, y) \phi_j(x, y) dx dy, \quad (\text{B.10})$$

just as in equations (4.17) and (5.18), for $j = 0, 1, 2$. \square

The proof is similar for higher order polynomials and more discontinuities.

Appendix C

Used Variables and Parameters

In the table below we summarize the variables and parameters that we have used in this article. We distinguish between five kinds of variables: grid, tracer distribution, mapping parameters, flux and advection distances and finally, mass.

Table of variables and parameters		
<i>variable</i>	<i>summary</i>	<i>dimension</i>
Grid		
N_{tot}	nr. gridcells	-
Δx	horizontal spacing	m
Δy	vertical spacing	m
Δt	timestep	s
i, j	cell number	-
Tracer distribution		
Φ	orthonormal basis	-
ϕ_n	elements of Φ	-
f	tracer distribution before mapping	kg
α	coefficients of f	-
\bar{f}	tracer distribution after mapping	kg
$\bar{\alpha}$	coefficients of \bar{f}	-
g	tracer distribution after LS	kg
β	coefficients of g	-
Mapping parameters		
λ, ξ	Lin-Map par's in x direction	-
ρ, ζ	Lin-Map par's in y direction	-
flux and advection		
A	flux	kg/s
d_L, d_U	relative advection distance for inflow	$[0, 1]$
e_L, e_U	relative advection distance for outflow	$[0, 1]$
Mass		
$m(t)$	air mass in a cell at time t	kg
$\Delta m_{low}, \Delta m_{up}$	net inflow masses	kg

Appendix D

Grids and the Earth

In the three figures D.1 - D.3 we illustrate the three grids we have discussed in the introduction. The first one is the regular grid, with very small cells near the poles (in terms of area). Then we have figure D.2 where some cells are added up together. This grid is still structured which is not optimal. Finally we have figure D.3 where we need lesser cells. This increases the speed of the model, but the advection step itself is more complicated than in case of a more structured grid like the reduced grid.

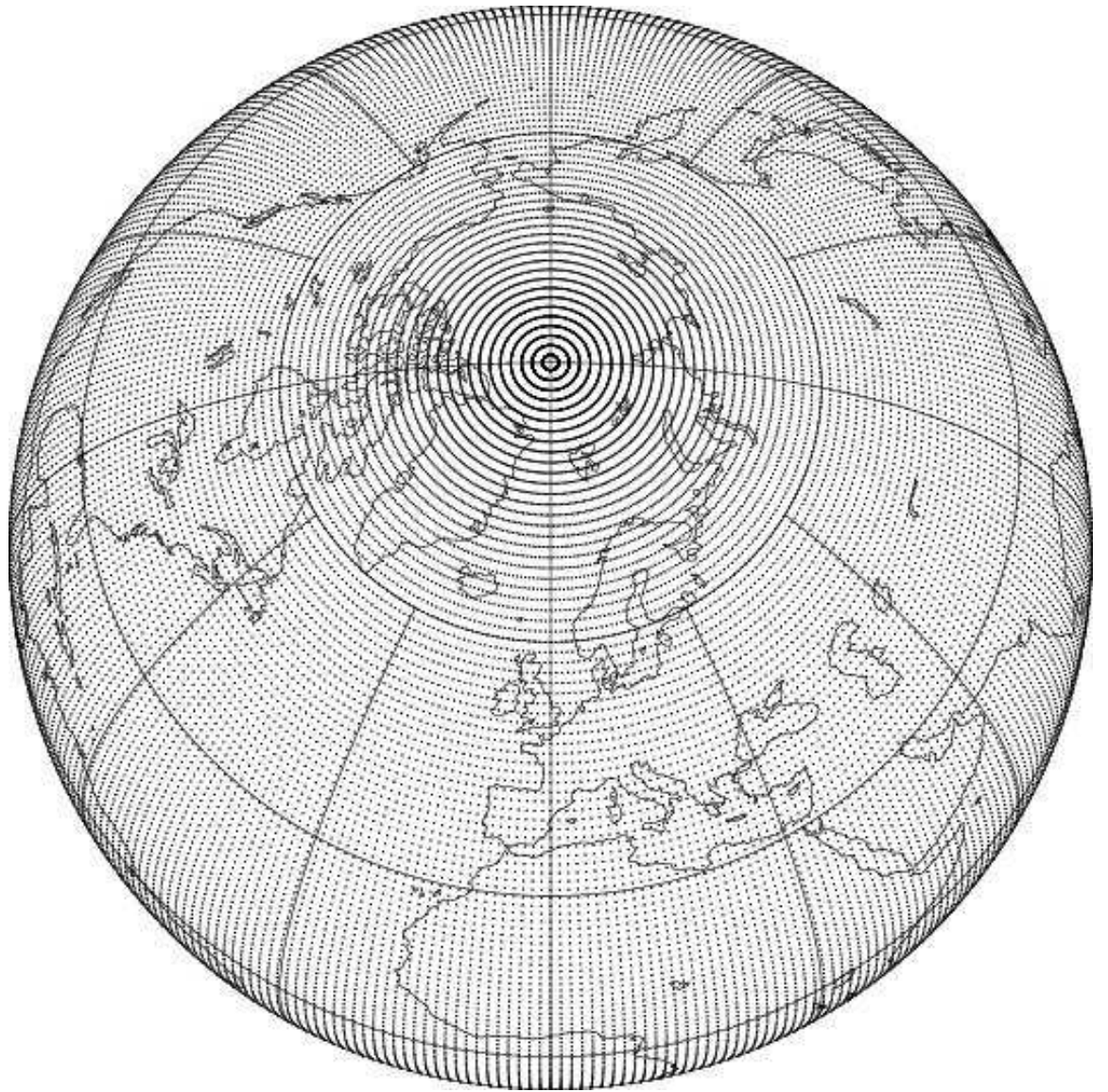


Figure D.1: The regular grid around the earth. The area of the gridcells becomes very small near the poles.

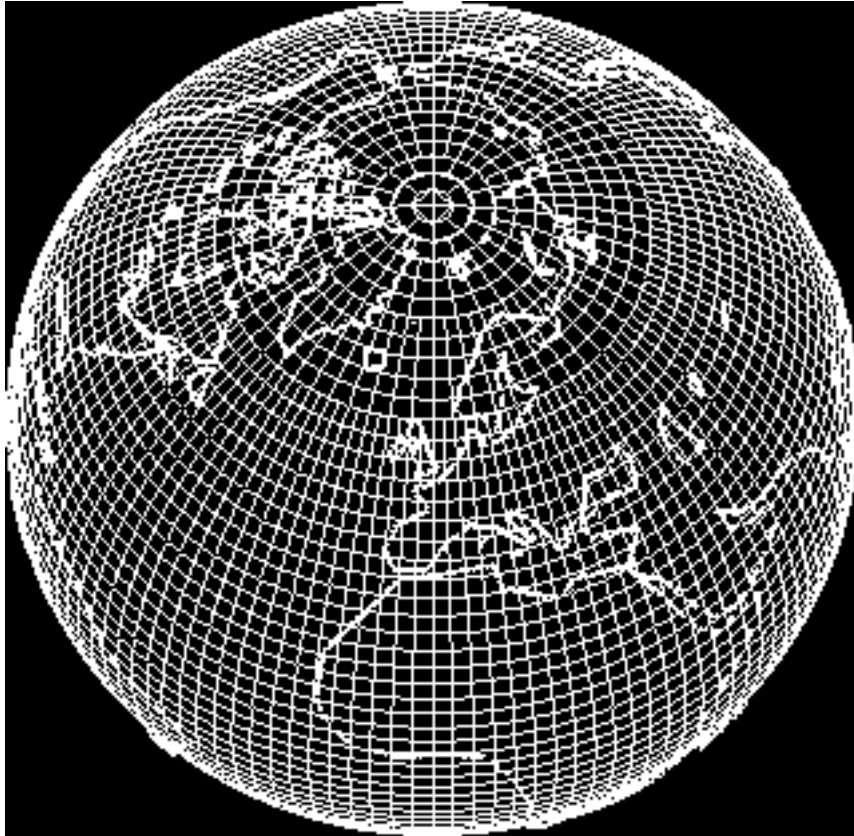


Figure D.2: The reduced grid around the earth. Cells are add up together to hold the grid structured and avoid very small cells.

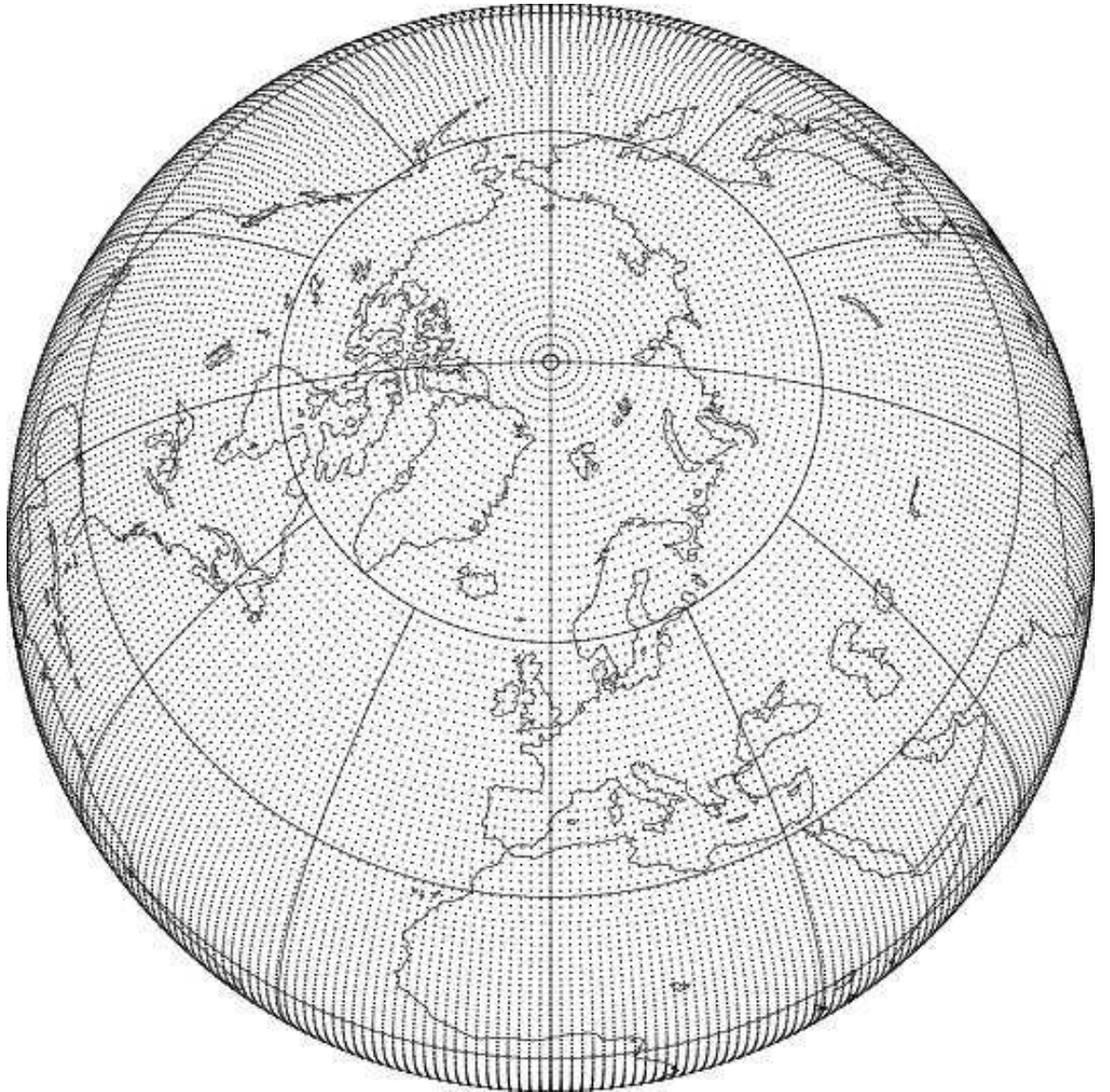


Figure D.3: The full reduced grid around the earth. Lesser cells are needed near the poles, which increases the simulation speed, since there are less iterations necessary.

Bibliography

- [Krol et al., 2005] Krol, M., Houweling, S., Bregman, B., van den Broek, M., Segers, A., van Velthoven, P., Peters, W., and Dentereen, F. (2005). The two-way nested global chemistry-transport zoom model tm5: algorithm and applications. *Atmos. Chem. Phys.*, 2:417–432.
- [Lanser and Verwer, 1999] Lanser, D. and Verwer, J. G. (1999). Analysis of operator splitting for advection-diffusion-reaction problems from air pollution modeling. *J. Comp. Appl. Math.*, 111:201–216.
- [Lay, 2003] Lay, D. C. (2003). *Linear Algebra and Its Applications*. Addison-Wesley, third edition.
- [Petersen et al., 1998] Petersen, A. C., Spee, E. J., van Dop, H., and Hundsdoerfer, W. (1998). An evaluation and intercomparison of four new advection schemes for use in global chemistry models. *J. Geophys. Res.*, 103:253–269.
- [Prather, 1986] Prather, M. (1986). Numerical advection by conservation of second-order moments. *J. Geophys. Res.*, 91:6671–6681.
- [Russell and Lerner, 1981] Russell, G. and Lerner, J. (1981). A new finite-differencing scheme for the tracer transport equation. *Journal of Applied Meteorology*, 20:1483–1498.

